Global distribution of ULF waves during magnetic storms:

Comparison of Arase, ground observations and BATSRUS+CRCM simulation

Naoko Takahashi[1], Kanako Seki[1], Mariko Teramoto[2], Mei-Ching Fok[3], Yihua Zheng[3], Ayako Matsuoka[4], Nana Higashio[5], Kazuo Shiokawa[2], Dmitry Baishev[6], Akimasa Yoshikawa[7], Tsutomu Nagatsuma[8]

1. Graduate School of Science, The University of Tokyo, Tokyo, Japan.
2. Institute for Space-Earth Environmental Research, Nagoya University, Nagoya, Japan.
3. NASA Goddard Space Flight Center, Greenbelt, Maryland, USA.
4. Institute of Space and Astronautical Science, Japan Aerospace Exploration Agency, Kanagawa, Japan.
5. Japan Aerospace Exploration Agency, Tsukuba, Japan.
6. Yu.G.Shafer Institute of Cosmophysical Research and Aeronomy, Siberian Branch of Russian Academy of Sciences, Yakutsk, Russia.
7. Department of Earth and Planetary Sciences, Faculty of Sciences, Kyushu University, Fukuoka, Japan
8. National Institute of Information Communications Technology, Tokyo, Japan

Reference:
Takahashi, N., et al. (2018), Global distribution of ULF waves during magnetic storms: Comparison of Arase, ground observations, and BATSRUS + CRCM simulation, *Geophysical Research Letters*, *45,* doi:10.1029/2018GL078857.

Radiation belt in the Earth's magnetosphere

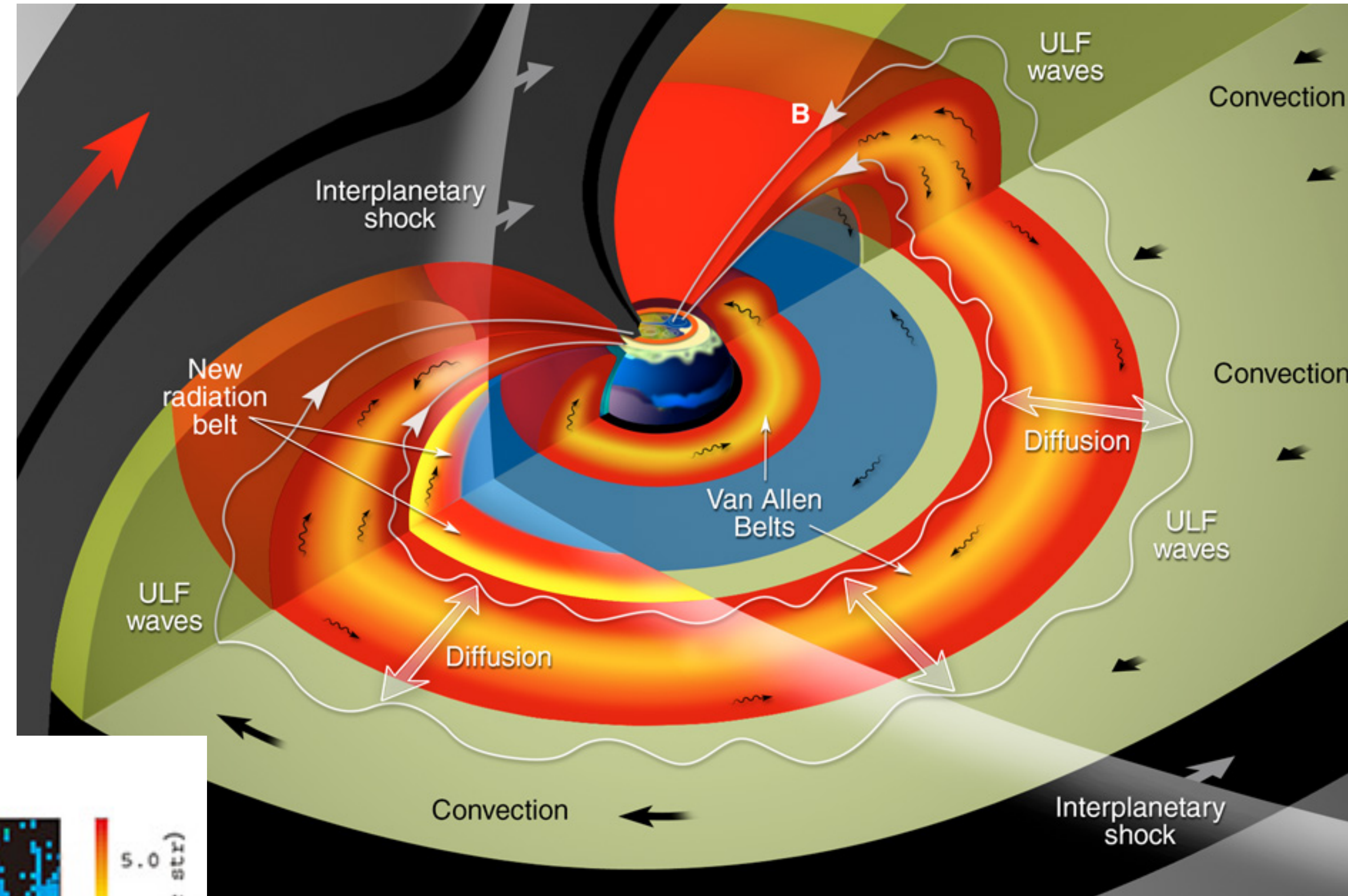

[Credit: NASA]

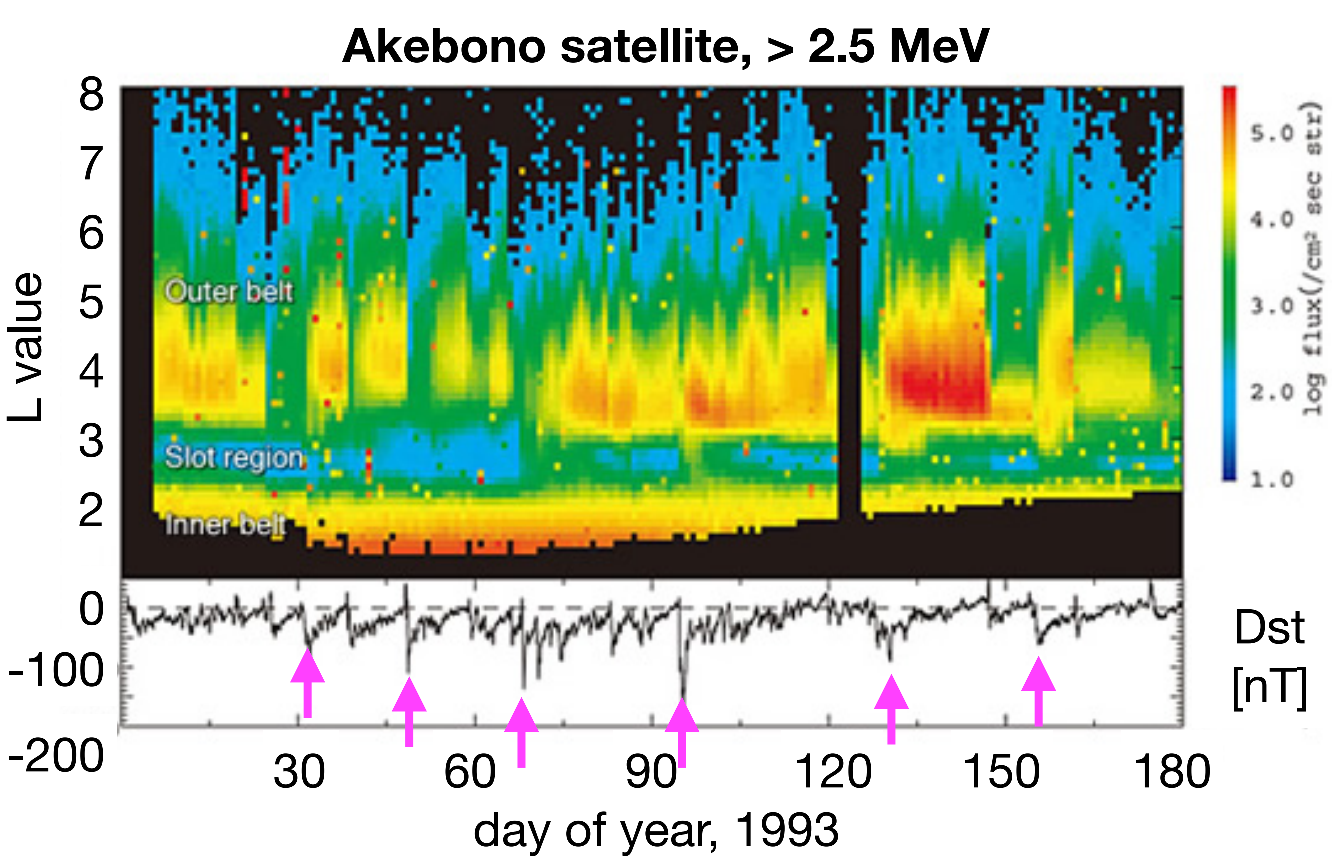

[Credit: ISAS news No.302]

- Relativistic electron fluxes in the outer radiation belt exhibit the dynamic activity of magnetic storms.
- Enhancement of high-energy electrons in the radiation belt

→ **When? Where? How?**

Electron acceleration: Non-adiabatic vs. Adiabatic

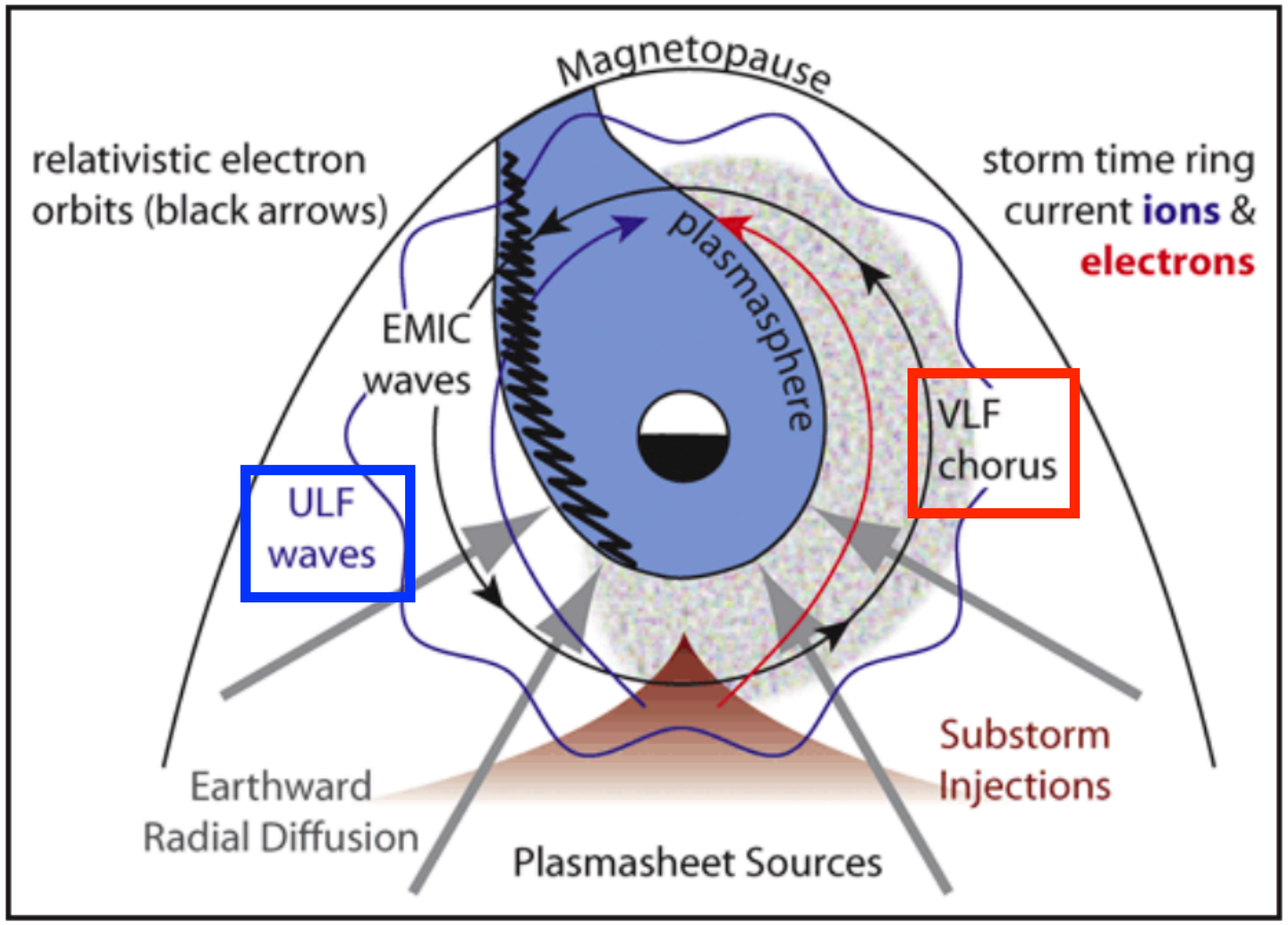

[Reeves, 2007]

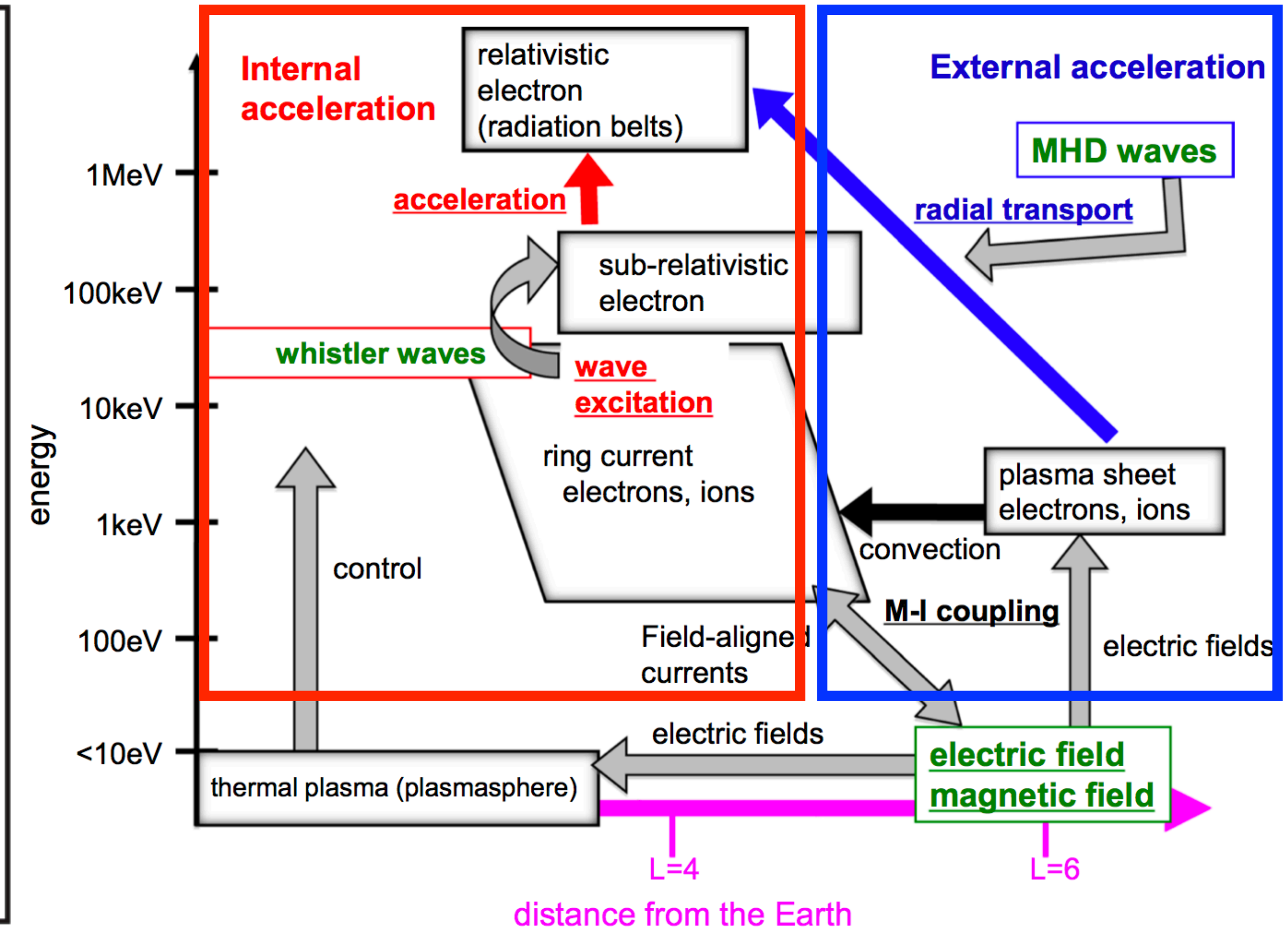

[Miyoshi et al., 2018]

acceleration of MeV electrons

1. **Internal acceleration (non-adiabatic): plasma waves (chorus waves)**
   → local acceleration by wave-particle interactions with whistler-mode chorus waves
2. **External supply (adiabatic): MHD waves (ULF waves)**
   → radial diffusion by ULF waves with periods of a few minutes

← **target of this study**

Pc5 ULF waves = Possible energy reservoir

- Frequency range: 1.6 – 6.7 mHz
  ⇔ Period: 150 – 600 s
- produce a radial diffusion of energetic particles

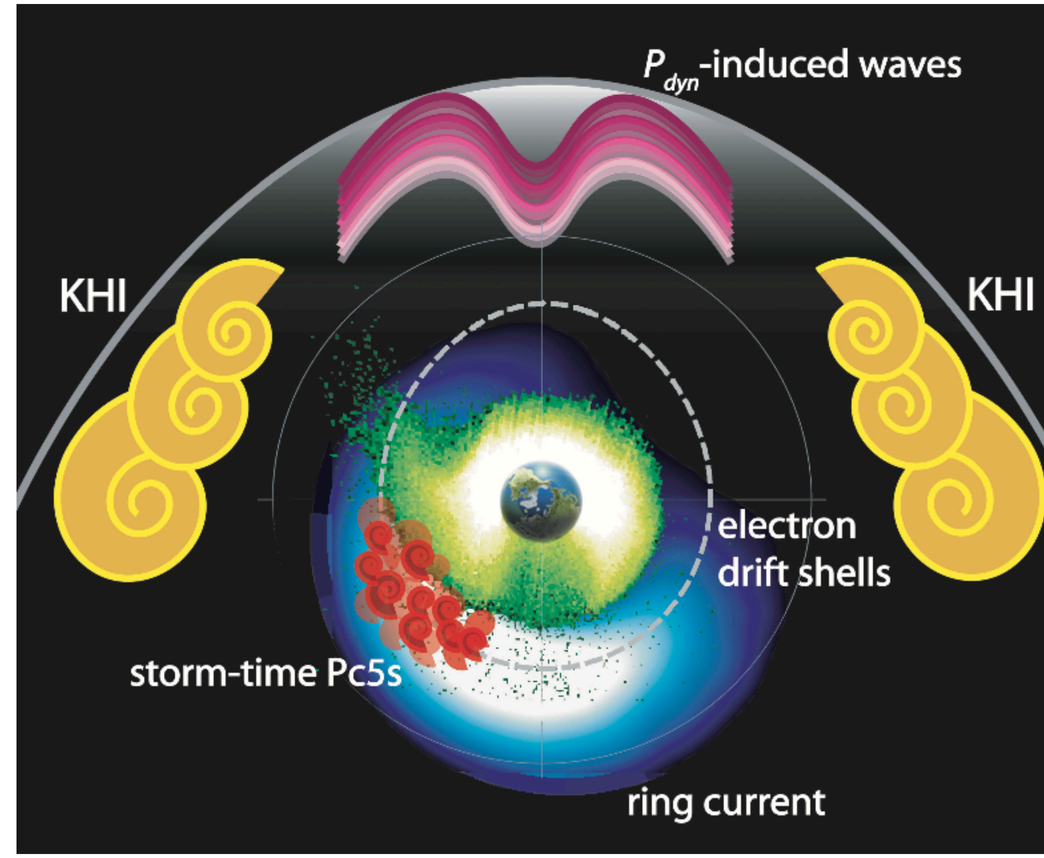

[Ukhorskiy et al., 2009]

classification of Pc5 pulsations

	Externally driven (solar wind driven)		Internally driven (storm-time Pc5)
driver	compression by solar wind	Kelvin-Helmholtz instability	ring current plasma by substorm injection
dominant component	toroidal (B_{phi} & E_r)		poloidal (B_r & E_{phi})
azimuthal wave number	low (≦10)		high (~40–120)
relate to…	solar wind dynamic pressure	bulk velocity of solar wind	substorm activity (AE index)
from ground magnetometers…	can be seen		cannot be seen

Global distribution of ULF waves

Observation: GMAG

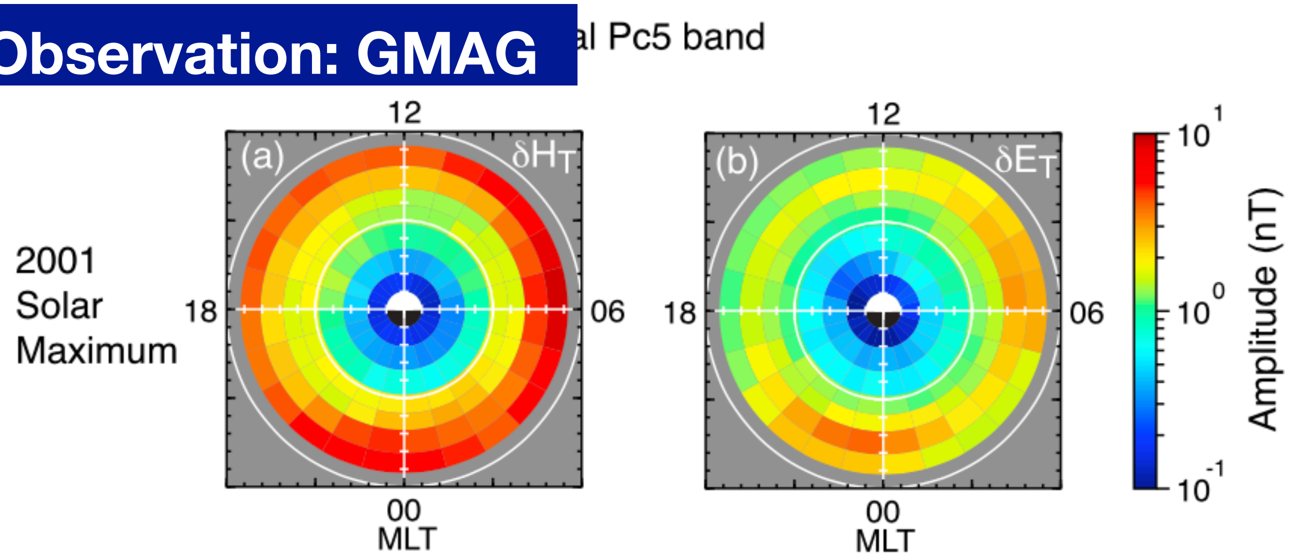

[K. Takahashi et al., 2012]

Simulation: BATSRUS+CIMI

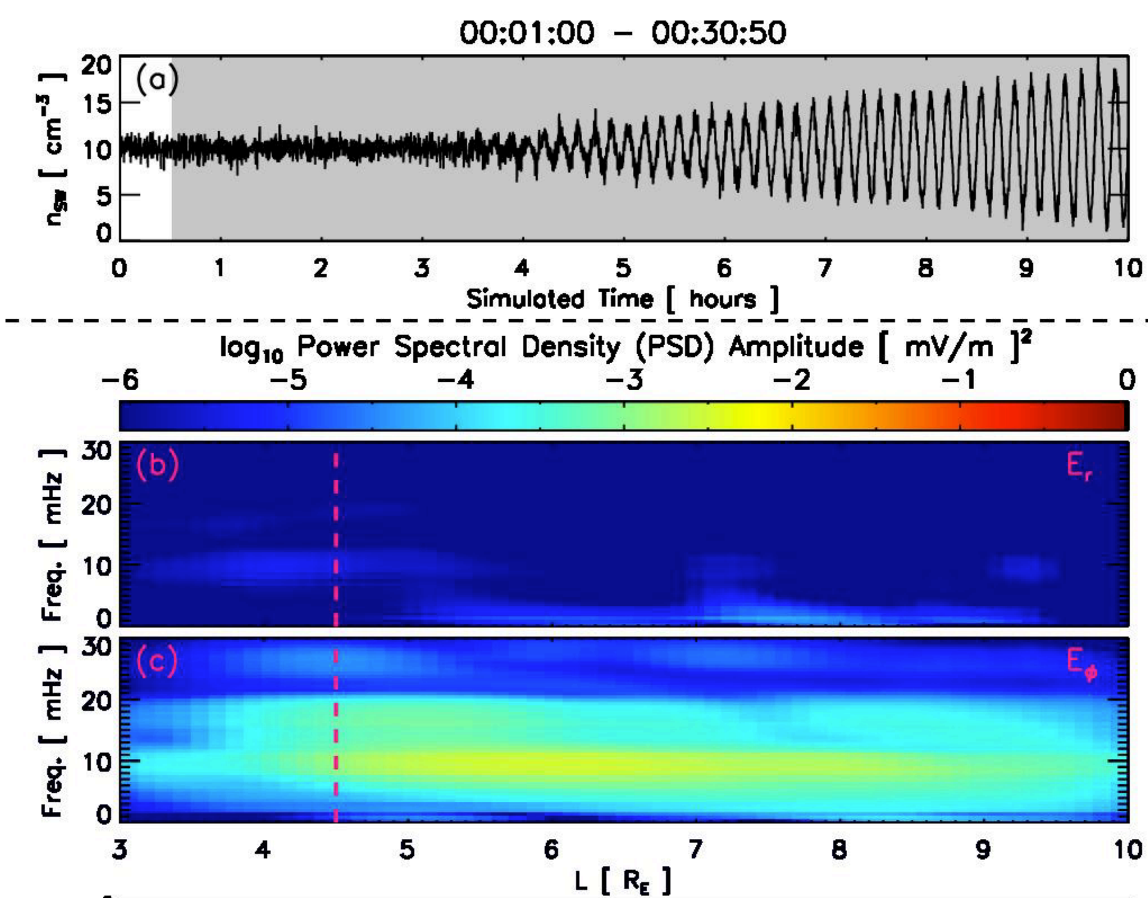

[Komar et al., 2017]

- The occurrence characteristics of ULF waves (i.e., dependence on SW parameters) have been statistically examined with ground and space observations [e.g., K. Takahashi et al., 2012].
- **Temporal variations in the global distribution of ULF waves during a specific storm event** have not been extensively studied with observations or simulation.

The comprehensive study using observations and numerical simulations makes essential and significant contributions.

Purpose

We compare the ULF wave activity during the specific storm between the simulation and the observation.

1. 'Local' comparison

MHD+RC model vs. direct measurement

- Can the simulation reproduce specific ULF waves observed by the Arase satellite?

2. 'Global' comparison

MHD+RC model vs. ground observations

- Can the simulation reproduce the global activity of ULF waves?
  → So far, we compare with the global activity derived from the ground magnetic field data.

27 March 2017 storm: CIR-type storm

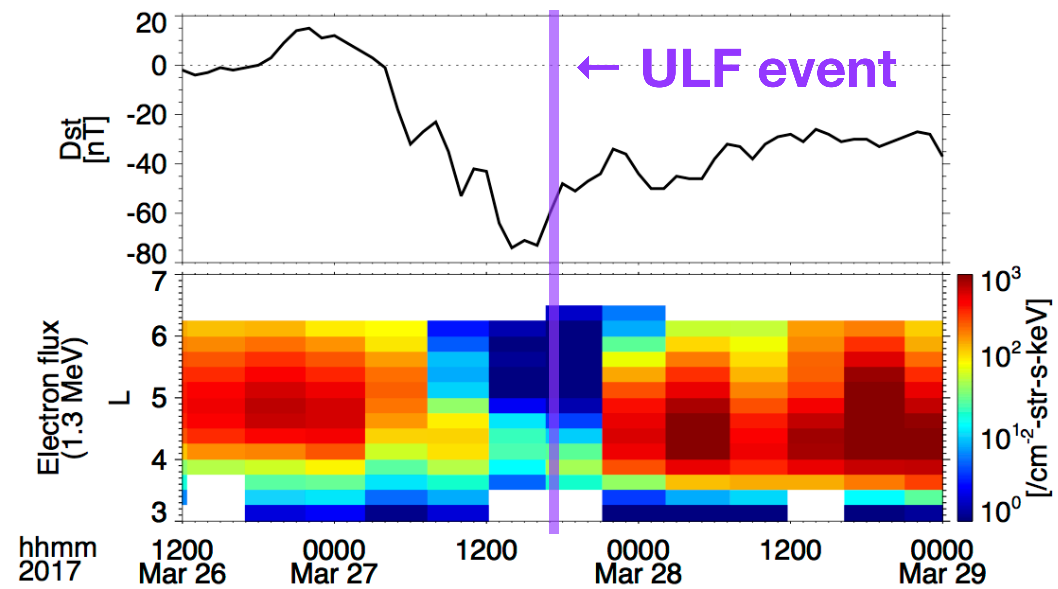

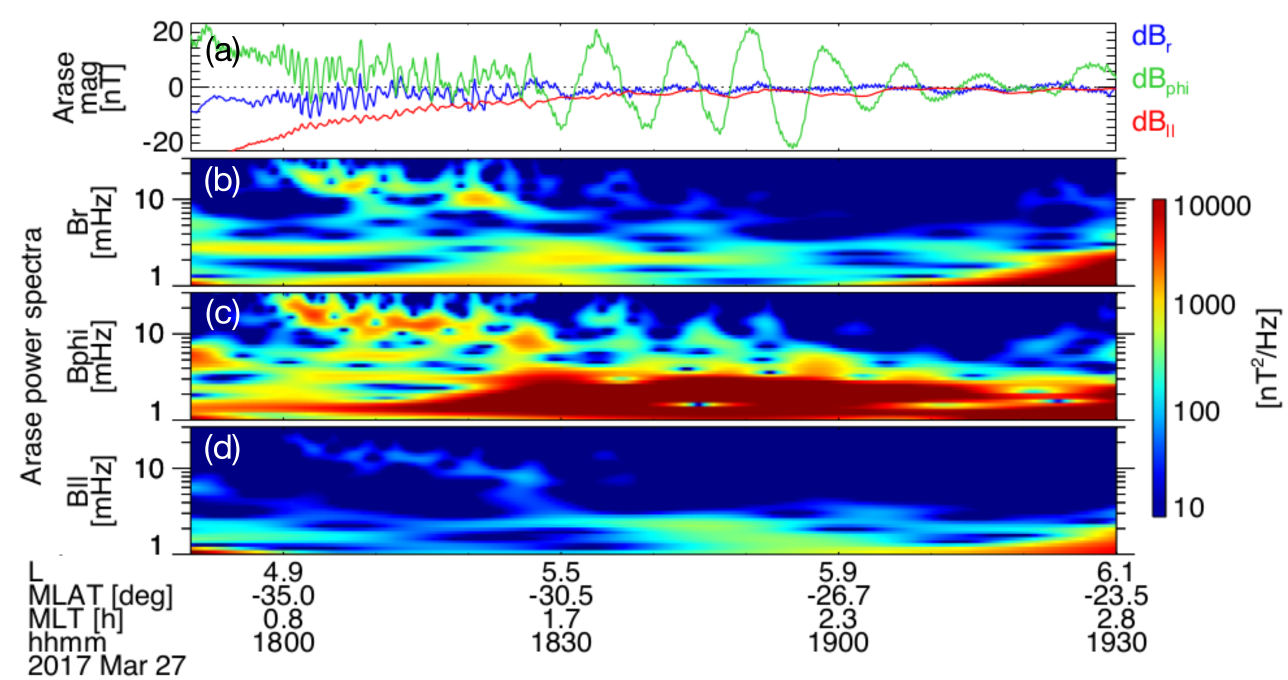

BATSRUS+CRCM

[coupling method: Buzulukova et al., 2010; Glocer et al., 2013]

Global magnetosphere: ideal MHD

BATS-R-US
(Block-Adaptive-Tree Solar-Wind Roe-Type Upwind Scheme)

[Powell et al., 1999]

continuity	$\frac{\partial \rho}{\partial t} + \mathbf{u} \cdot \nabla \rho + \rho \nabla \cdot \mathbf{u} = 0$	Faraday's law	$\mathbf{j} = \frac{1}{\mu_0} \nabla \times \mathbf{B},$
momentum	$\rho \frac{\partial \mathbf{u}}{\partial t} + \rho \mathbf{u} \cdot \nabla \mathbf{u} + \nabla \mathbf{p} - \mathbf{j} \times \mathbf{B} = 0,$	Ampere's law	$\frac{\partial \mathbf{B}}{\partial t} + \nabla \times \mathbf{E} = 0,$
heat balance	$\frac{\partial p}{\partial t} + \mathbf{u} \cdot \nabla \mathbf{p} + \gamma \mathbf{p} \nabla \cdot \mathbf{u} = 0,$	Ohm's law	$\mathbf{E} = -\mathbf{u} \times \mathbf{B},$

Pressure ↑ ↓ magnetic field momentum

electric potential conductivity ↑ ↓ current

Inner magnetosphere: ring current model

CRCM
(Comprehensive Ring Current Model)

[Fok et al., 2001]

bounce-averaged Boltzmann equation

$$\frac{\partial \bar{f}_s}{\partial t} + \langle \dot{\lambda} \rangle \frac{\partial \bar{f}_s}{\partial \lambda} + \langle \dot{\phi} \rangle \frac{\partial \bar{f}_s}{\partial \phi} = -\mathrm{v}\sigma_s \langle \mathrm{n_H} \rangle \bar{f}_s - \left(\frac{\bar{f}_s}{0.5\tau_b} \right)_{loss\ cone}$$

$$\bar{f}_s = \bar{f}_s(\lambda, \phi, M, K)$$

Ionosphere

Ionospheric electrodynamics

← potential

map back to magnetosphere (@2.5 R_E) using background B

We have requested data with the high-time resolution (10 sec) to CCMC.

Initial condition

Simulation box size

- 32 R_E (upstream)~224 R_E (downstream)
- cartesian grid:
  finest: 0.25 R_E in the inner magnetosphere ($|x, y, z| \leqq 15$ R_E)

Solar wind input condition

- Only IMF Bx is fixed (average).
- The dipole tilt is included (~5.09° in X-Z plane).

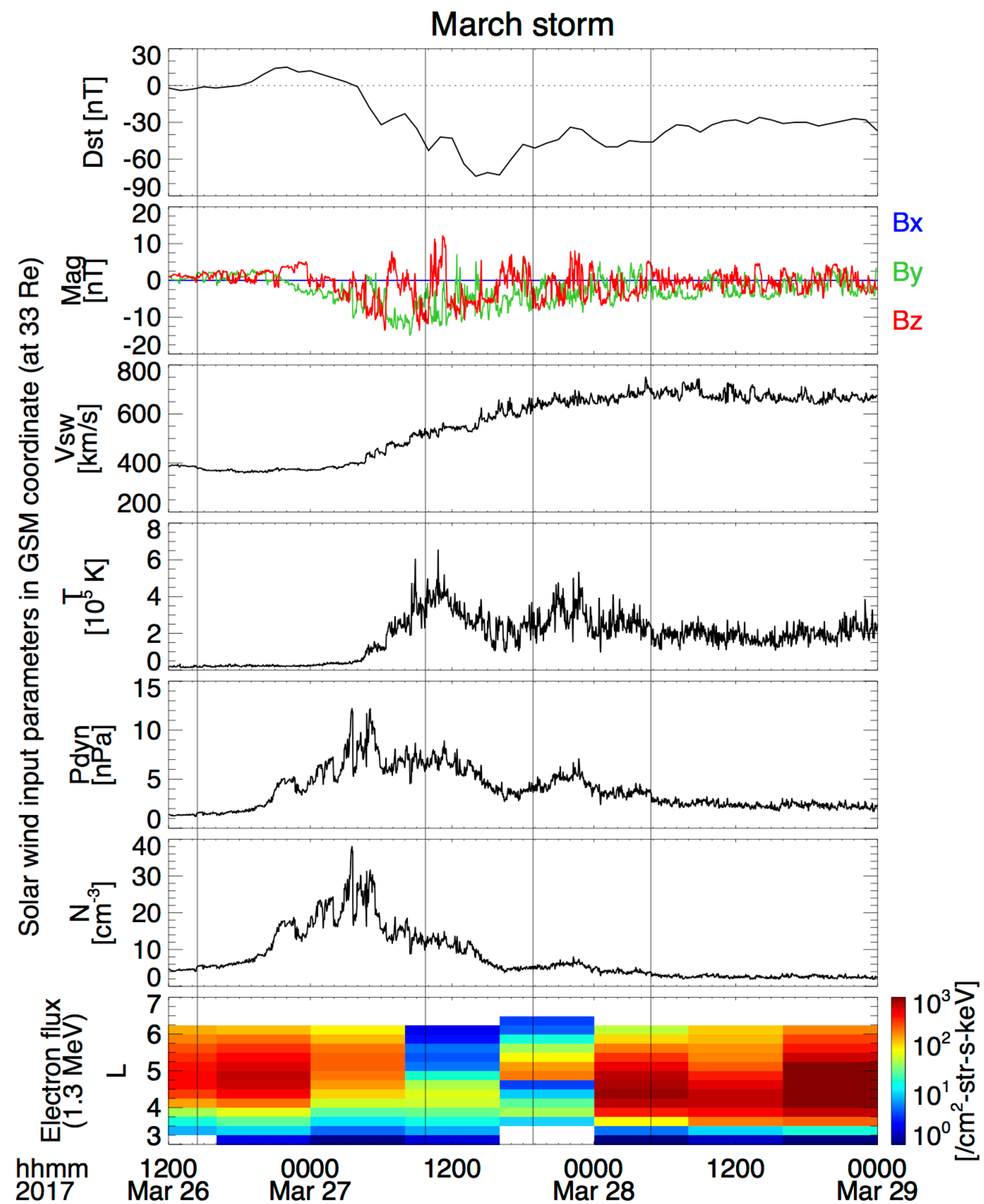

Boundary

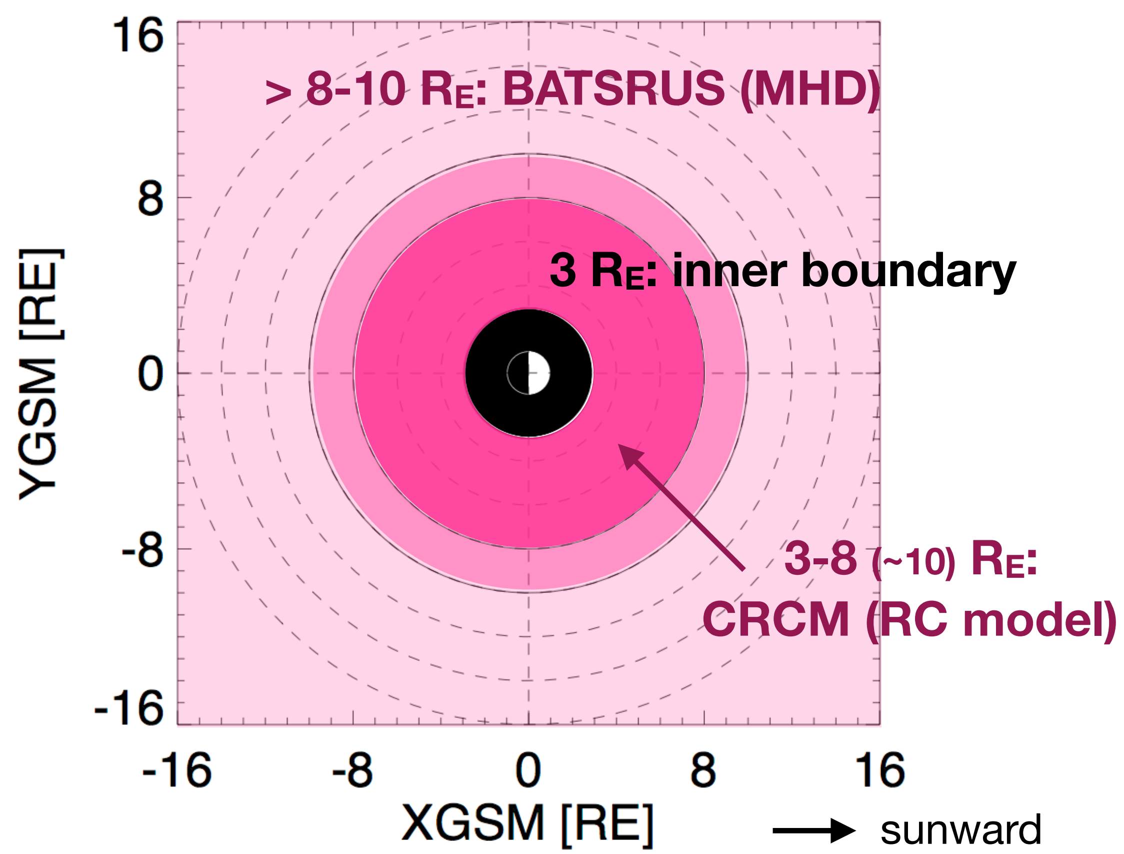

Global distribution (@Z=0 plane, +/- 15 R_E)

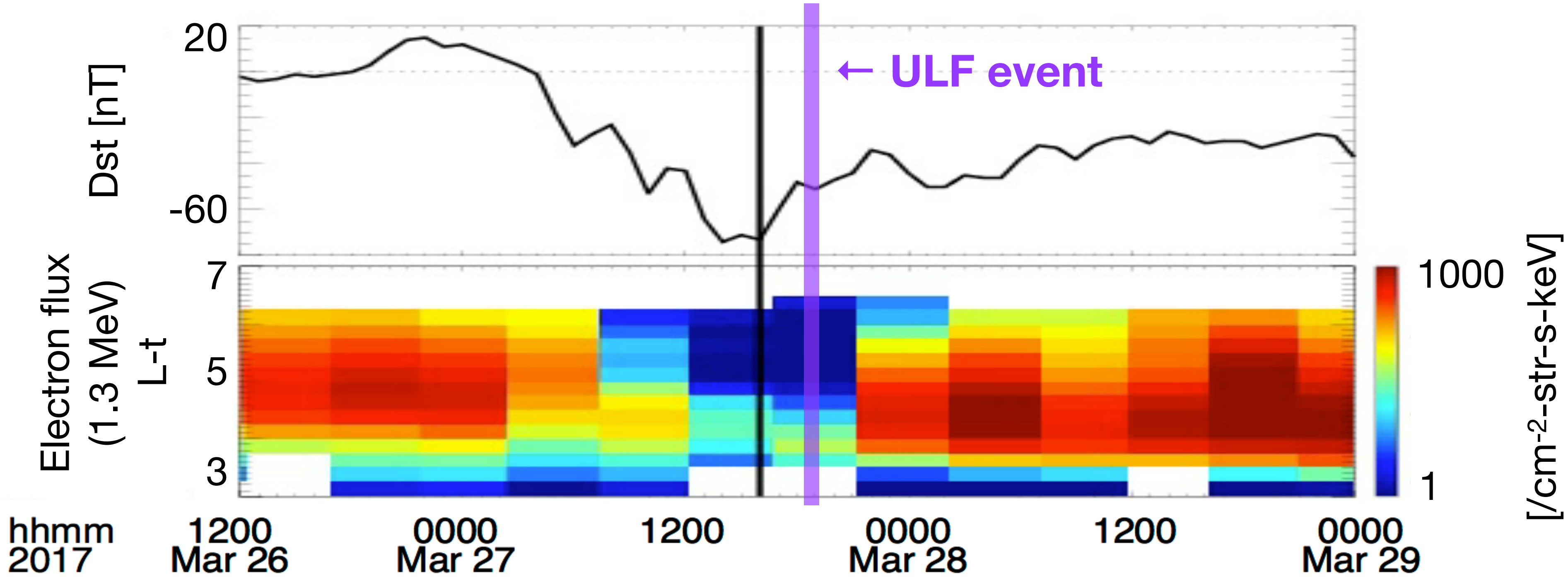

total pressure & flow velocity

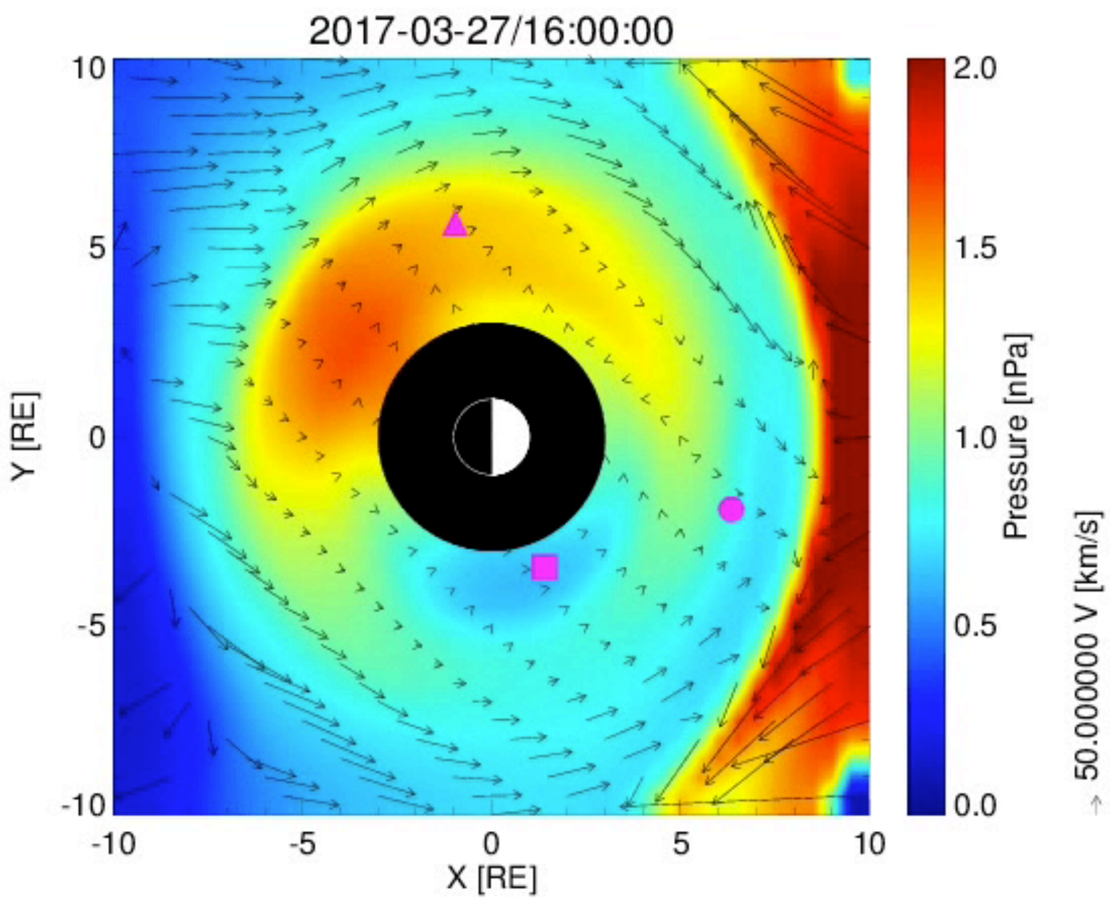

ULF wave power in toroidal component (B_{phi})

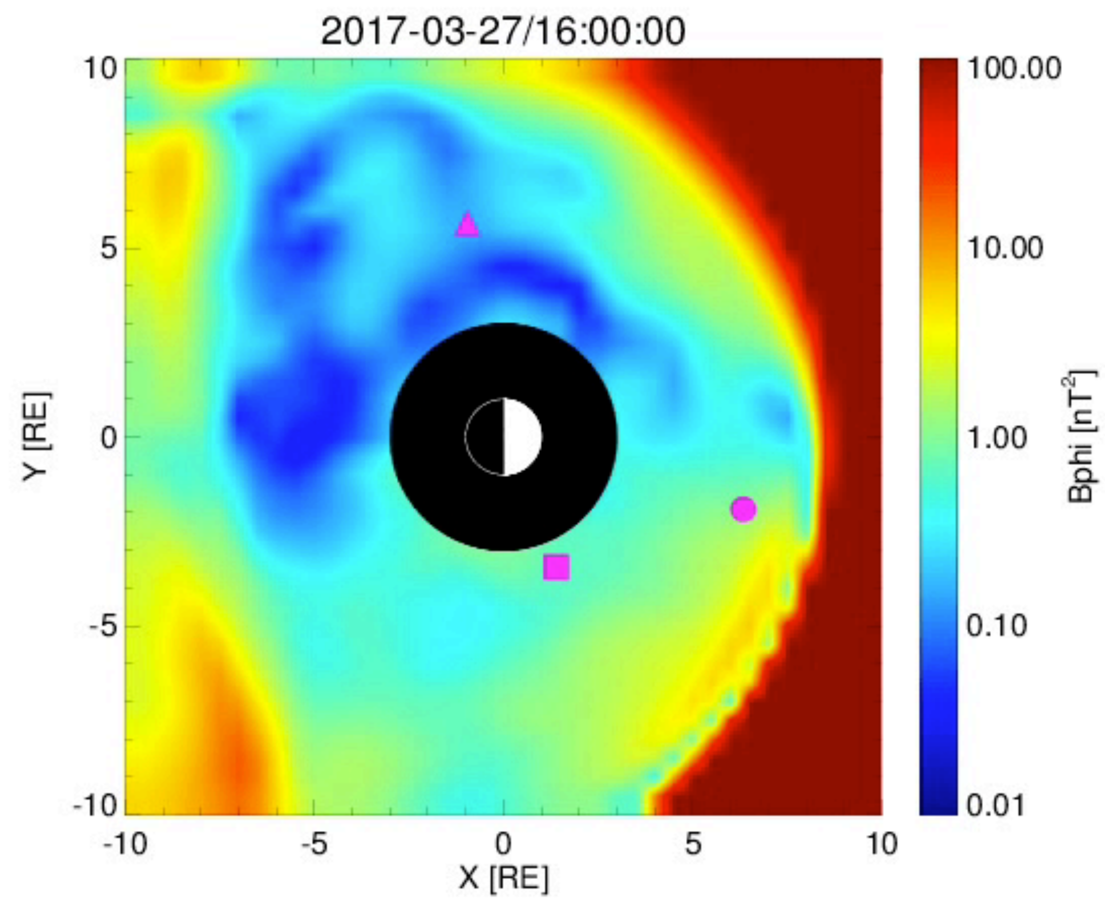

■ Arase

Global distribution (@Z=0 plane, +/- 15 R_E)

pre-storm **main phase** **ULF event (early recovery)** **recovery phase**

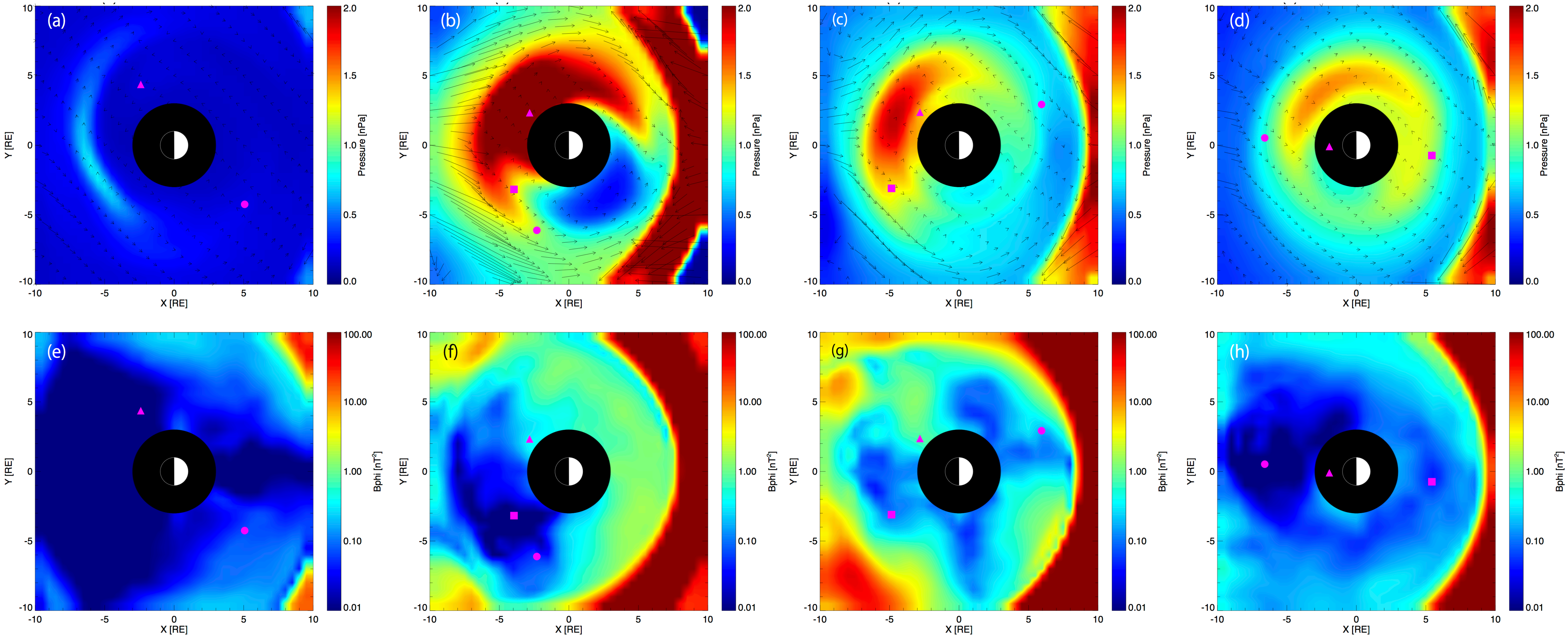

(upper) total pressure & flow velocity
(lower) integrated power in B_{phi} (toroidal component): over Pc5 frequency range

- asymmetric distribution of total pressure
  → corresponds to the partial ring current
- a four-packet structure of ULF wave power during the early recovery phase
  → **Low-*m* ULF waves (*m*~4) = external-driven ULF waves**

‘Local’ comparison: Simulation vs. The Arase satellite

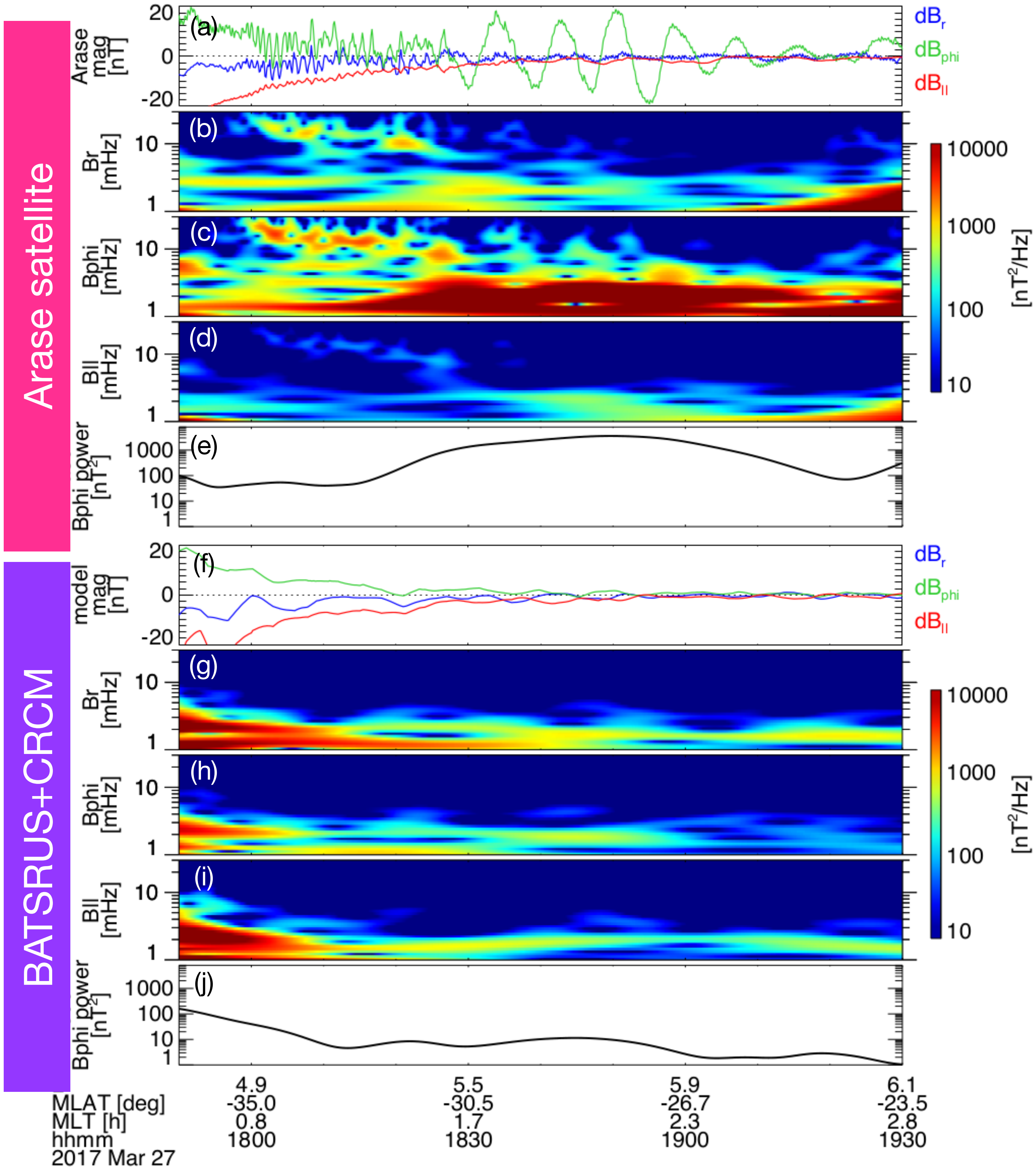

The simulation can reproduce the enhancement of ULF waves in B_{phi} (frequency: 2-3 mHz).
→ **consistent with Arase**

Discrepancies

- smaller amplitude of ULF waves
  → large numerical dissipation
- different characteristics of wave power in $B_{||}$ (waveform: similar)
  → different magnetic field configuration due to the Cartesian grid
- No higher-frequency waves (10-30 mHz)
  → low temporal resolution of solar wind input parameters (~1 min)

*background: 15-min running average

‘Global’ comparison: Simulation vs. GMAG

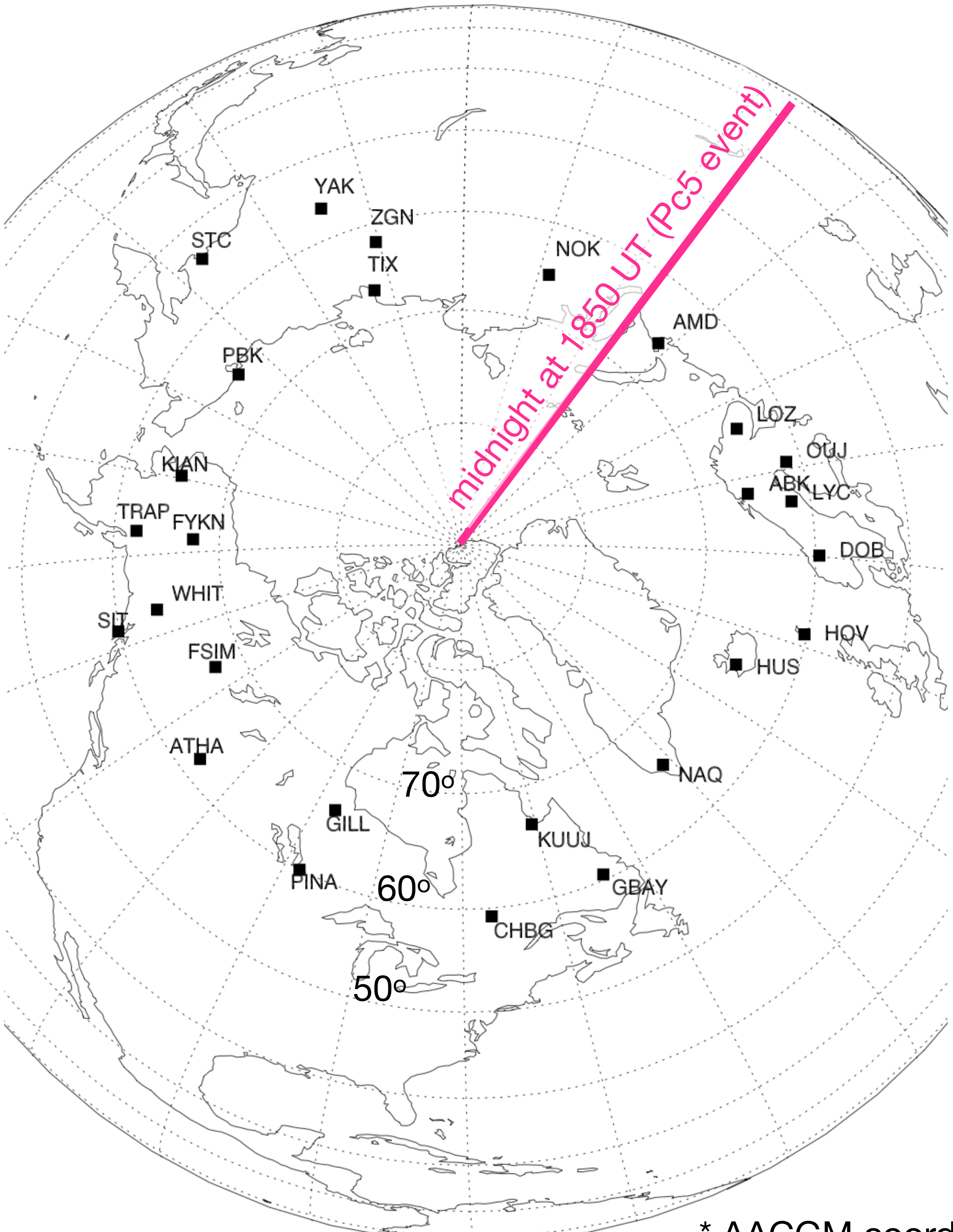

* AACGM coord.

- GMAG location: MLAT = 54o – 68o
  → roughly corresponds to L = 3.5 – 7.0 at the magnetospheric equatorial plane

- We calculated **the root-integrated power (RIP)** [Claudepierre et al., 2016].

$$RIP = \left[\int_{f_{low}}^{f_{high}} PSD(f)df \right]^{\frac{1}{2}}$$

f_{low}=0.016 Hz
f_{high}=0.067 Hz
PSD: power spectral density

- The calculated RIP of ULF waves is normalized by 3-h average during the pre-storm time.
  → **especially focus on the relative activity level**

‘Global’ comparison: Relative ULF activity

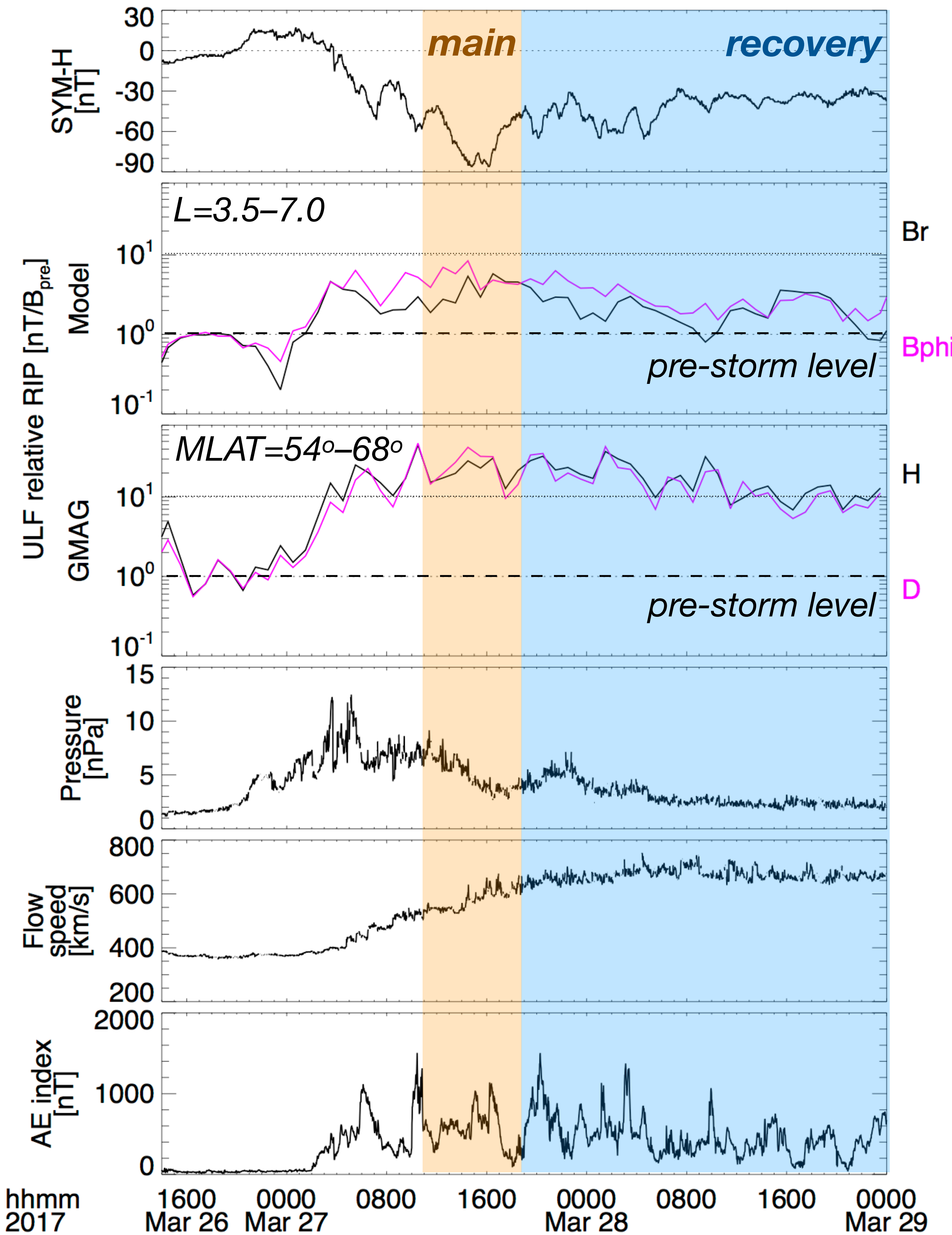

The simulated ULF wave activity is **strongly** affected by the solar wind dynamic pressure.

Pc5-range ULF wave activity

	simulation	GMAG
main	high	high
	↓	↓
recovery	(relatively) low	high
relate to…	**pressure**	**pressure + V_{SW} & AE**

The ULF wave activity on the ground may include the effects of the KH instability and/or substorms.

* ULF wave intensity:
normalized by 3-h average during the pre-storm

Question:

What type of ULF waves can BATSRUS+CRCM reproduce?

classification of Pc5 pulsations

	Externally driven		Internally driven
driver	compression by solar wind	Kelvin-Helmholtz instability	ring current plasma by substorm injection
relate to…	solar wind dynamic pressure	bulk velocity of solar wind	AE index (substorm activity)

Answer:
only driven by the compression of the magnetosphere by the solar wind

Kelvin-Helmholtz instability

- large numerical dissipation in BATSRUS+CRCM
- If the grid resolution is partially increased, KHI will be seen in the model.
  cf. LFM global model [Claudepierre et al., 2007]: partially increase at the flank (0.125 R_E)

Substorm injection

- The bounce-averaged approach may miss short-time scale phenomena [Glocer et al., 2013]

Summary

1. BATSRUS+CRCM can qualitatively reproduce ULF waves observed by the Arase satellite.

Discrepancy between the simulation and the observation

- The amplitude of simulated magnetic field is underestimate.
  → mainly due to a large numerical dissipation in BATSRUS+CRCM code
- Higher frequency waves (10–30 mHz) cannot be reproduced.
  → low temporal resolution of input parameters (~1 min)

2. BATSRUS+CRCM is suitable for Pc5 ULF waves driven by the compression of the magnetosphere by the solar wind.

Comparing with the ULF wave activity on the ground

- The ground ULF wave activity may include KH instabilities and/or substorm activities.

Contribution to the study using SuperDARN

- The global map of ionospheric flows can be easily derived from SuperDARN.
  → **Comparison of the global map between in the ionosphere and in the magnetosphere helps us for the further understanding the energy transfer during the magnetic storm.**

Thank you for your attention!

Acknowledgement

- BATSRUS+CRCM modeling
  Community Coordinated Modeling Center at Goddard Space Flight Center through their public Runs on Request system (https://ccmc.gsfc.nasa.gov)

- Arase satellite
  - Magnetic field experiment (MGF): v.01.00 data
  - Extremely high energy electron experiment (XEP): v.01.00 data generated on 8 August 2017 partly supported by the SEES/JAXA
  - The authors are deeply grateful to the entire ERG (Arase) project team for developing each instrument and performing the calibration.

- Solar wind parameter & geomagnetic indices:
  World Data Center for Geomagnetism, Kyoto (http://wdc.kugi.kyoto-u.ac.jp)

- Ground magnetometers:
  - Dr. Alexander Pashinin and Dr. Nozomu Nishitani
  - THEMIS-GBO
  - National Institute of Polar Research
  - Technical University of Denmark
  - Tromsø Geophysical Observatory
  - Geological Survey of Sweden
  - Finnish Meteorological Institute
  - AARI in Russia
  - The authors also appreciate INTERMAGNET for promoting high standards of magnetic observatory practice (www.intermagnet.org).